Chemistry and Physics of Lipids 219 (2019) 28–35

Contents lists available at ScienceDirect

Chemistry and Physics of Lipids

journal homepage: www.elsevier.com/locate/chemphyslip

The apoA-I mimetic peptide 4F protects apolipoprotein A-I from oxidative damage

C. Roger White[a], Geeta Datta[a], Landon Wilson[c], Mayakonda N. Palgunachari[a], G.M. Anantharamaiah[a,b,*,1]

[a] Department of Medicine, University of Alabama at Birmingham, Birmingham, AL, 35294, United States
[b] Department of Biochemistry and Molecular Genetics, University of Alabama at Birmingham, Birmingham, AL, 35294, United States
[c] Targeted Metabolomics and Proteomics Laboratory, University of Alabama at Birmingham, Birmingham, AL, 35294, United States

ARTICLE INFO

Keywords:
ApoA-I
ApoA-I mimetic peptide
Hypochlorous acid
Oxidation
Cholesterol efflux

ABSTRACT

High density lipoprotein (HDL) is prone to modification by the oxidizing and chlorinating agent hypochlorite anion (OCl^-). Oxidation of apolipoprotein (apo) A-I, the major protein in HDL, reduces ABCA-1 mediated cholesterol efflux and other protective responses to HDL. The apoA-I mimetic peptide 4F has been shown to undergo oxidation; however, the ability of the peptide to mediate cholesterol efflux remains intact. Here, we show that 4F protects apoA-I from hypochlorite-mediated oxidation. Mass spectral analysis of apoA-I shows that tyrosine residues that are prone to hypochlorite-mediated chlorination are protected in the presence of 4F. Furthermore, 4F enhances the cholesterol efflux ability of apoA-I to a greater extent than either 4F or apoA-I alone, even after hypochlorite oxidation. These observations suggest that apoA-I in lipid complexes may be protected by the presence of 4F, resulting in the preservation of its anti-inflammatory and anti-atherogenic properties. These studies also form the basis for the future studies of nanoparticles possessing both apoA-I and 4F.

1. Introduction

High density lipoproteins (HDL) are anti-atherogenic and protect the artery wall from cholesterol buildup (Rye et al., 2009; Gorden et al., 1977). The proposed mechanisms for this protection include its ability to efflux cholesterol from cells and anti-oxidant properties. Several laboratories have shown that cellular cholesterol efflux by itself triggers cell signaling processes that inhibit inflammation (White et al., 2014). Apolipoprotein (apo) A-I, the major protein component of HDL, has also been shown to inhibit lesion formation in animal models of atherosclerosis (Navab et al., 2011a). Several preclinical and clinical studies have been performed using apoA-I:lipid complexes and apoA-I variants such as apoA-I_{Milano}:lipid complexes (Shah et al., 2001). However, while animal studies have shown efficacy of apoA-I -phospholipid nanoparticles for reducing atherosclerosis, encouraging results have not been obtained in human trials (Nissen et al., 2003; Tardif et al., 2007; Shaw et al., 2008). Thus, investigations for obtaining synthetic HDL that is effective in humans have continued.

Synthetic HDL-like nanoparticles derived from apoA-I can deliver molecules directly to the cytoplasm of certain cancer cells, effectively bypassing the endosomal compartment (Kenneth et al., 2011). This strategy could allow HDL-like nanoparticles to be used to deliver drugs that have increased activity in the cytoplasm. Lipoprotein nanoparticles have evolved to be ideal delivery vehicles, and, because of that specialized function, they have the potential to improve therapies for diseases such as atherosclerosis and cancer (Nissen et al., 2003; Tardif et al., 2007; Shaw et al., 2008; Kenneth et al., 2011; Ibanez et al., 2012). Nanodisc system has also been used for both the discovery of new pharmacological agents as well as the therapeutic delivery of small molecule and protein based therapeutics (Jin et al., 2010; Zhang et al., 2009; Skajaa et al., 2010).

ApoA-I interacts with phospholipids to form peptide:lipid complexes. While apoA-I forms discoidal complexes with 1,2-dimyristoyl *sn*-glycerophospho choline (DMPC) spontaneously, detergents are needed for apoA-I to form nanoparticles with 1-Palmitoyl-2-oleoyl-*sn*-glycero-3-phosphocholine (POPC). Lipid free apoA-I interacts with ABCA1 on the cell surface and forms apoA-I-phospholipid nanoparticles, which in turn pick up cellular cholesterol for delivery to the liver, a process termed reverse cholesterol transport (Kingwell et al., 2014). However, apoA-I present in these nanoparticles is prone to oxidative modification

* Corresponding author at: 1022 Zeigler Research Building, Birmingham, AL, 35294-0007, United States.
E-mail address: Ananth@uab.edu (G.M. Anantharamaiah).
[1] G.M. Anantharamaiah is a principal for Bruin Pharma.

https://doi.org/10.1016/j.chemphyslip.2019.01.009
Received 5 October 2018; Received in revised form 10 January 2019; Accepted 28 January 2019
Available online 29 January 2019
0009-3084/

(Anantharamaiah et al., 1988). This may change anti-inflammatory HDL into pro-inflammatory (Van Lenten et al., 1995). We have studied apoA-I mimetic peptides extensively, in particular, peptide 4F (Navab et al., 2010). 4F spontaneously interacts with oxidized lipids, a property apoA-I does not exhibit (Van Lenten et al., 2008). This property of 4F is thought to be responsible for its ability to inhibit lesion formation in several animal models (Navab et al., 2011b; Reddy et al., 2013; Navab et al., 2008). The peptide 4F has been shown to ameliorate several lipid-mediated disorders including atherosclerosis, Alzheimer's disease and diabetes (White et al., 2014). Furthermore, treatment of 4F with the oxidizing and chlorinating agent hypochlorite anion (OCl^-) results in the modification of a tryptophan (Trp) residue without affecting other properties of the peptide (White et al., 2012). 4F also interacts with eggPC and POPC vesicles to produce clear solution (Datta et al., 2001). Based on these observations, we hypothesized that 4F protects apoA-I from oxidative modification. In this report, we show that the presence of 4F protects apoA-I from hypochlorite-mediated oxidation. Furthermore, presence of 4F enhanced the ability of apoA-I to efflux cellular cholesterol, thus forming the basis for study of nanoparticles containing 4F-apoA-I and POPC.

2. Methods

2.1. Materials

1-Palmitoyl-2-oleoyl-*sn*-glycero-3-phosphocholine (POPC) was purchased from Avanti Polar Lipids, Inc. (Alabaster, AL). Sodium hypochlorite was from Sigma, Inc. Superose 6 columns were from Amersham Biosciences (NJ, USA). ^{3}H-cholesterol was from American Radiochemicals (St Louis, Mo). Hypochlorite concentration was determined by monitoring absorbance at 292 nm ($\varepsilon = 350 M^{-1} cm^{-1}$) in 0.1 N NaOH using a Shimadzu Spectrophotometer Model UV-2501PC. See Blue Plus 2 low molecular weight markers were from InVitrogen, Inc.

2.2. Peptide and apoA-I purification

The apoA-I mimetic peptide 4F, whose amino acid sequence is Ac-DWFKAFYDKVAEKFKEAF-NH_2 (2310 mw), was synthesized by the solid phase peptide synthesis method as previously described (Datta et al., 2001). Peptide purity was determined by mass spectral analysis and analytical HPLC. The concentration for 4F was determined using $\varepsilon_{280} = 7300 M^{-1} cm^{-1}$. Human apoA-I was purified from plasma obtained from American Red Cross donors, as previously described (Anantharamaiah et al., 1988). Briefly, HDL was isolated from plasma by density gradient centrifugation (Chung et al., 1996). After delipidation and lyophilization of HDL, apoA-I was purified by preparative HPLC on a reverse-phase column (Anantharamaiah and Garber, 1996). ApoA-I purity was determined by mass spectrometry and SDS gel electrophoresis. ApoA-I concentration was determined using $\varepsilon_{280} = 31{,}500\ M^{-1}/cm^{-1}$.

2.3. Electrophoresis studies

ApoA-I was analyzed by denaturing gel electrophoresis in order to determine whether hypochlorite modifies physical characteristics of the apolipoprotein. Hypochlorite anion is a strong oxidizing agent that rapidly reacts with physiological substrates. Hypochlorite (43–129 μM) was added to apoA-I (100 μg/mL) dissolved in PBS (pH 7.4) for 15 min. This did not significantly alter the pH of the reaction solution. Residual hypochlorite activity was quenched by the addition of 100 μM taurine. Native and hypochlorite-modified apoA-I (15 μg) was then loaded onto a 4–20% SDS-Tris glycine gel and stained with Coomassie blue. Gels were scanned, and band density was assessed using LabWorks software (Lablogics, Inc. V4.6).

2.4. Mass spectrometry

Reaction products of apoA-I and hypochlorite (and their modification by 4F) were assessed by mass spectrometry. Samples of apoA-I (100 μg/mL) and hypochlorite (129 μM) were prepared in the presence and absence of 4F (100 μg/mL). These were loaded onto an SDS gel and separated as described above. Bands were then excised from the gels and subjected to tryptic digest. Sequence analysis of the tryptic fragments was performed using NanoLC-tandem mass spectrometry. An aliquot (2 μL) of each digest was loaded onto a 2 cm × 75μm i.d. PepMap100 C_{18} reverse-phase trap cartridge (Dionex, Sunnyvale) at 2 μL/min using an Eksigent autosampler. After washing the cartridge for 4 min with 0.1% formic acid in double-distilled H_20, the bound peptides were flushed onto a 15 cm × 75 μm i.d. PepMap100 C_{18} reverse-phase analytical column (Dionex, Sunnyvale, CA) with a 40 min linear (5–50%) acetonitrile-H_2O gradient in the presence of 0.1% formic acid at 300 nl/min using an Eksigent Nano1D + LC. (Dublin, CA). The column was washed with 90% acetonitrile-0.1% formic acid for 15 min and then re-equilibrated with 5% acetonitrile-0.1% formic acid for 30 min.

The Applied Biosystems 5600 Triple-TOF mass spectrometer (AB-Sciex, Toronto, Canada) was used to analyze the peptide digest. Eluted peptides were subjected to a time-of-flight survey scan from 400 to 1250 *m/z* to determine the top twenty most intense ions for MS/MS analysis. Product ion time-of-flight scans at 50 ms were carried out to obtain the tandem mass spectra of the selected parent ions over the range from *m/z* 400–2000. Spectra were centroided and de-isotoped by Analyst software, version TF (Applied Biosystems). A β-galactosidase trypsin digest was used to establish and confirm the mass accuracy of the mass spectrometer.

2.5. Cholesterol efflux

ABCA1-dependent cholesterol efflux was measured following the procedure of Kritharides et al. (1998). THP-1 monocytes were seeded at 10^6 cells/well in 6-well plates and differentiated to a macrophage phenotype by addition of phorbol 12-myristate 13-acetate (20 nM). cAMP was then added to cells for 24 h to induce ABCA1 expression. Acetylated LDL, radiolabeled with [^{3}H]cholesterol, was added to cells for 24 h at 37 °C. Cells were then incubated with 100 μg/mL apoA-I for 24 h at 37 °C. In some experiments, hypochlorite (43, 86 and 129 μM) was added to apoA-I prior to addition to THP-1 cells. After 24 h, media and cell lysates were collected for [^{3}H]cholesterol scintillation counting to determine amount of cholesterol effluxed from cells. We also monitored the effects of hypochlorite on apoA-I -mediated cholesterol efflux in the presence of 4F (100 μg/mL). As before, hypochlorite (46–129 μM) was added to the apoA-I /4F reaction mixture for 15 min, followed by addition of taurine. Data are presented as the percentage of total counts effluxed into the culture medium.

2.6. Measurement of apoA-I-4F-POPC particle size

Non-denaturing gradient gel electrophoresis (4–20%) was used to further characterize apoA-I -4F-POPC complexes, as previously described (Sorci-Thomas et al., 1997). Complex size was determined using protein markers of known Stokes radii. The bands were identified by silver staining.

2.7. Crosslinking of apoA-I and 4F

To assess whether 4F and apoA-I are situated in close proximity in the POPC complexes, crosslinking using bis(sulfosuccinimidyl) suberate (BS^3) was carried out using the procedure of D'Silva et al. (2005). Briefly, 6.5 mg/ml of BS^3 was added to apoA-I-4F-POPC complexes at a protein to crosslinker ratio of 1:10. Hydrolysis of BS^3 was minimized by rapid addition of the crosslinker to the complexes, followed by

incubation at 4 °C for 24 h. The reaction was terminated by adding Tris – HCl at a final concentration of 100 mM. SDS gel electrophoresis (4–20% gel) of the crosslinked sample along with apoA-I was carried out. The gel was stained with Coomassie blue and the bands excised and the presence of 4F examined by mass spectrometry.

2.8. Phospholipid clarification

The effect of 4F and apoA-I on the clarification of POPC was determined by following the dissolution of POPC multi-lamellar vesicles (MLVs) by right angle light scattering using an SLM 8000C photon counting spectrofluorometer, as described previously (Datta et al., 2004). POPC MLVs were prepared by evaporating a solution of POPC under nitrogen and hydrating the lipid film with phosphate-buffered saline (pH 7.4). The sample containing 0.9 mM POPC and 1 mg apoA-I was maintained at 25 °C and continuously stirred. Addition of 4F resulted in clarification of the POPC MLVs. Different apoA-I:4F (w/w) ratios were used, maintaining POPC amount same in all of the experiments. 1 mg of 4F alone was added to POPC as a positive control. Turbidity clarification was monitored at 400 nm for 30 min at 25 °C.

2.9. Statistical methods

All results are reported as the mean ± SEM. Statistical analysis was performed using SigmaPlot 10 software (Systat Software, Inc.). Differences between the groups were assessed by one-way analysis of variance (ANOVA) with *post hoc* testing (Student-Neuman-Keuls test). A P value < 0.05 was considered statistically significant.

3. Results

Since previous studies show that hypochlorite oxidatively modifies apoA-I, we hypothesized that this reaction may be modified in the presence of 4F. In initial studies, apoA-I was exposed to increasing concentrations of hypochlorite and then resolved on SDS gels. As shown in Fig. 1A, the band density for apoA-I was reduced with increasing concentration of hypochlorite. Addition of 43μM hypochlorite yielded an apoA-I adduct with an approximate mass of 60 kD. At higher concentrations of hypochlorite, this band was further degraded (Fig. 1A). Addition of 4F to the apoA-I/hypochlorite reaction mixture prevented the oxidative degradation of apoA-I (Fig. 1B). Under these conditions, higher molecular weight adducts of apoA-I were formed with increasing hypochlorite concentration, a process well documented in the literature (Aeschbach et al., 1976). ApoA-I band densities were determined by densitometry and are depicted in Fig. 1C. The bar graph shows that apoA-I band density was significantly reduced with increasing hypochlorite concentration. Addition of 4F to the reaction mixture, however, attenuated the hypochlorite-mediated reduction in apoA-I density. These data show that 4F inhibits the hypochlorite-mediated oxidation of apoA-I.

Mass spectral analysis was performed to determine whether 4F modulates the reaction products formed by apoA-I and hypochlorite. ApoA-I (100 μg/mL) was mixed with hypochlorite (129 μM) in the presence and absence of 4F (100 μg/mL). Hypochlorite is a potent oxidizing and chlorinating agent. We found that the principal modification of apoA-I by hypochlorite is to induce the chlorination of tyrosine (Y) residues. Analysis of tryptic fragments of apoA-I showed that 5 tyrosine residues in the amino acid sequence for apoA-I were chlorinated by hypochlorite (Fig. 2, Table 1). Further, one of these residues (Y166) could also be dichlorinated (Table 1). Addition of 4F to the apoA-I /hypochlorite reaction mixture reduced the total number of chlorination sites in apoA-I by 50%. The chromatographic profile for the tryptic fragment VQPYLDDFQK is shown in Fig. 3A. The peak intensity for the fragment associated with hypochlorite-treated apoA-I was significantly reduced when apoA-I was exposed to hypochlorite in the presence of 4F. The chromatogram further shows that the level of unmodified apoA-I was negligible (Fig. 3A). MS analysis of the VQPYLDDFQK fragment associated with the hypochlorite-treated apoA-I peak

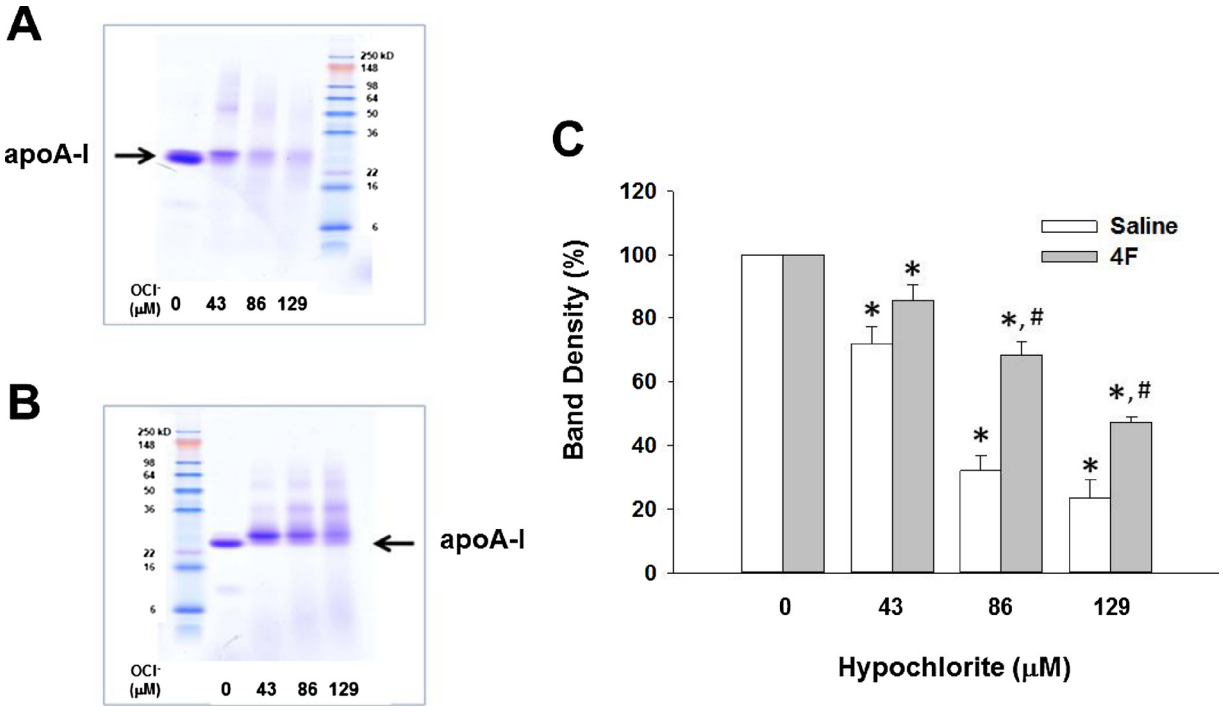

Fig. 1. 4F reduces the hypochlorite-dependent degradation of apoA-I. Addition of increasing concentrations of hypochlorite (OCl^-) reduced apoA-I band density when separated on an SDS-PAGE gel. (Panel A). Co-incubation of 4F and apoA-I and hypochlorite attenuates the hypochlorite-mediated reduction in apoA-I band density. (Panel B). Compiled data from SDS gels showing that 4F prevents the hypochlorite-mediated degradation of apoA-I. Data are the mean ± SEM for N = 7 gels. * denotes a significant difference ($P < 0.05$) compared to band density in the absence of hypochlorite. # denotes a significant difference ($P < 0.05$) compared to band density in the absence of 4F (Panel C).

DEPPQSPWDRVK**DLATVYVDVLK**DSGR**DYVSQFEGSALGK**QLNLKLLDNW
DSVTSTFSKLREQLGPVTQEFWDNLEKETEGLRQEMSKDLEEVKAK**VQPY**
LDDFQKKWQEEMELYRQKVEPLRAELQEGARQKLHELQEKLSPLGEEMRD
RARAHVDALR**THLAPYSDELR**QRLAARLEALKENGGARLAEYHAKATEHL
STLSEKAKPALEDLRQGLLPVLESFK**VSFLSALEEYTK**KLNTQ

Fig. 2. Sites of hypochlorite-dependent modification in apoA-I. ApoA-I was treated with hypochlorite and separated by SDS gel electrophoresis. Bands were excised and subjected to tryptic digestion. Five fragments were identified by mass spectrometry that contained chlorinated tyrosine (Y) residues. The fragments are presented in boldface type, and modified tyrosine residues are underlined.

Table 1
Hypochlorite chlorinates multiple tyrosine residues in apoA-I. ApoA-I was treated with hypochlorite (149μM) and resolved on an SDS gel. The band was excised and subjected to tryptic digestion. Mass spectrometry analysis revealed the presence of chlorinated tyrosine (Y) residues in six tryptic fragments of apoA-I.

Peptide Fragment	Modification	Residue	*m/z* Ratio	Charge State
DLATVYVDVLK	Chlorinated	Y18	635.328	2+
DYVSQFEGSALGK	Chlorinated	Y29	717.820	2+
VQPYLDDFQK	Chlorinated	Y100	643.796	2+
THLAPYSDELR	Chlorinated	Y166	445.876	3+
THLAPYSDELR	Dichlorinated	Y166	457.195	3+
VSFLSALEEYTK	Chlorinated	Y236	710.842	2+

yielded a molecule with an *m/z* ratio corresponding to 643.7989 Da (Fig. 3B). Additional isotopes containing one or two ^{13}C atoms were also observed in the MS spectrum. MS/MS sequence analysis of the principal peak confirmed that the tyrosine residue was chlorinated at position 100 (Y100) (Fig. 4). These data demonstrate that 4F attenuates the modification of apoA-I by hypochlorite. In addition to these modifications, as shown by the formation of higher molecular weight adducts, apoA-I also undergoes dimerization, as reported previously (Aeschbach et al., 1976).

We next monitored effects of hypochlorite on ABCA1-dependent cholesterol efflux in response to 4F and apoA-I. 4F or apoA-I (both 100 μg/mL) was mixed with hypochlorite (0–129 μM) as described above and then added to THP-1 macrophages that were pre-loaded with [^{3}H]-cholesterol. Treatment with hypochlorite did not alter 4F-mediated cholesterol efflux (Fig. 5). This result is in agreement with our previous findings (White et al., 2012). In contrast, treatment of apoA-I with 86 and 129 μM hypochlorite significantly reduced cholesterol efflux compared to apoA-I treated with saline vehicle (Fig. 5). In additional experiments, we measured efflux in cells that were exposed to apoA-I in the presence of 4F. Cholesterol efflux was almost doubled compared to treatment of cells with either 4F or apoA-I alone (Fig. 5). Interestingly, the reduction in apoA-I efflux at higher concentrations of

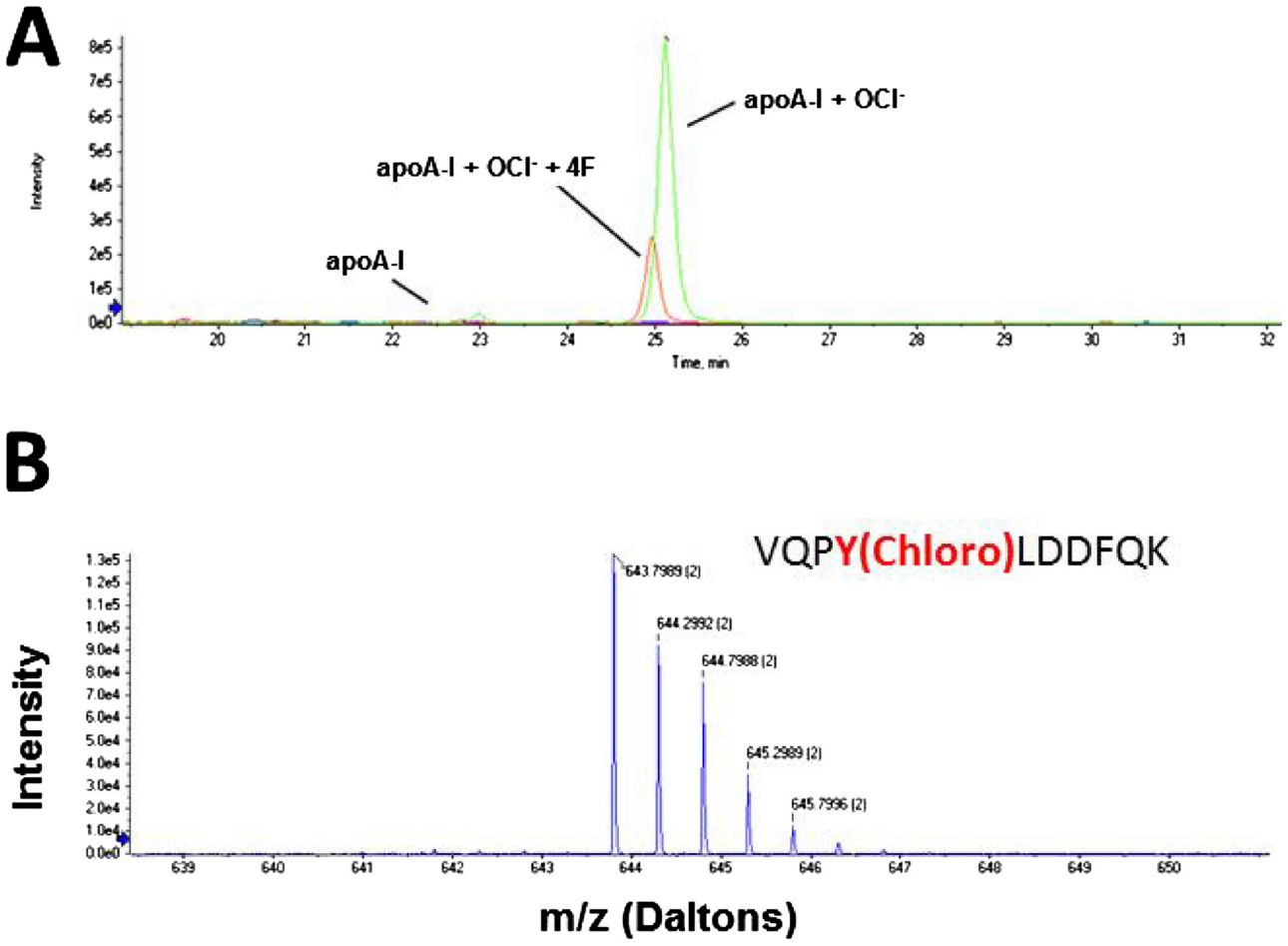

Fig. 3. 4F prevents the oxidative modification of apoA-I. Tryptic fragments of apoA-I were generated by the addition of hypochlorite (OCl^-) and eluted by chromatography. The fragment VQPYLDDFQK containing a chlorinated tyrosine residue is depicted in Panel A. Addition of 4F to this reaction mixture significantly reduced formation of this oxidized product. Levels of unmodified apoA-I were negligible. The MS spectrum for the chlorinated VQPYLDDFQK fragment is shown in Panel B. This fragment displays an isotopic distribution with double-charged tryptic fragments.

b				y	y^{+2}
---	1	V	10	---	---
228.1343	2	Q	9	1187.5134	594.2603
325.1870	3	P	8	1059.4548	530.2311
522.2114	4	Y (33.961)	7	962.4021	481.7047
635.2954	5	L	6	765.3777	383.1925
750.3224	6	D	5	652.2937	326.6505
865.3493	7	D	4	537.2667	269.1370
1012.4177	8	F	3	422.2398	211.6235
1140.4763	9	Q	2	275.1714	138.0893
---	10	K	1	147.1128	74.0600

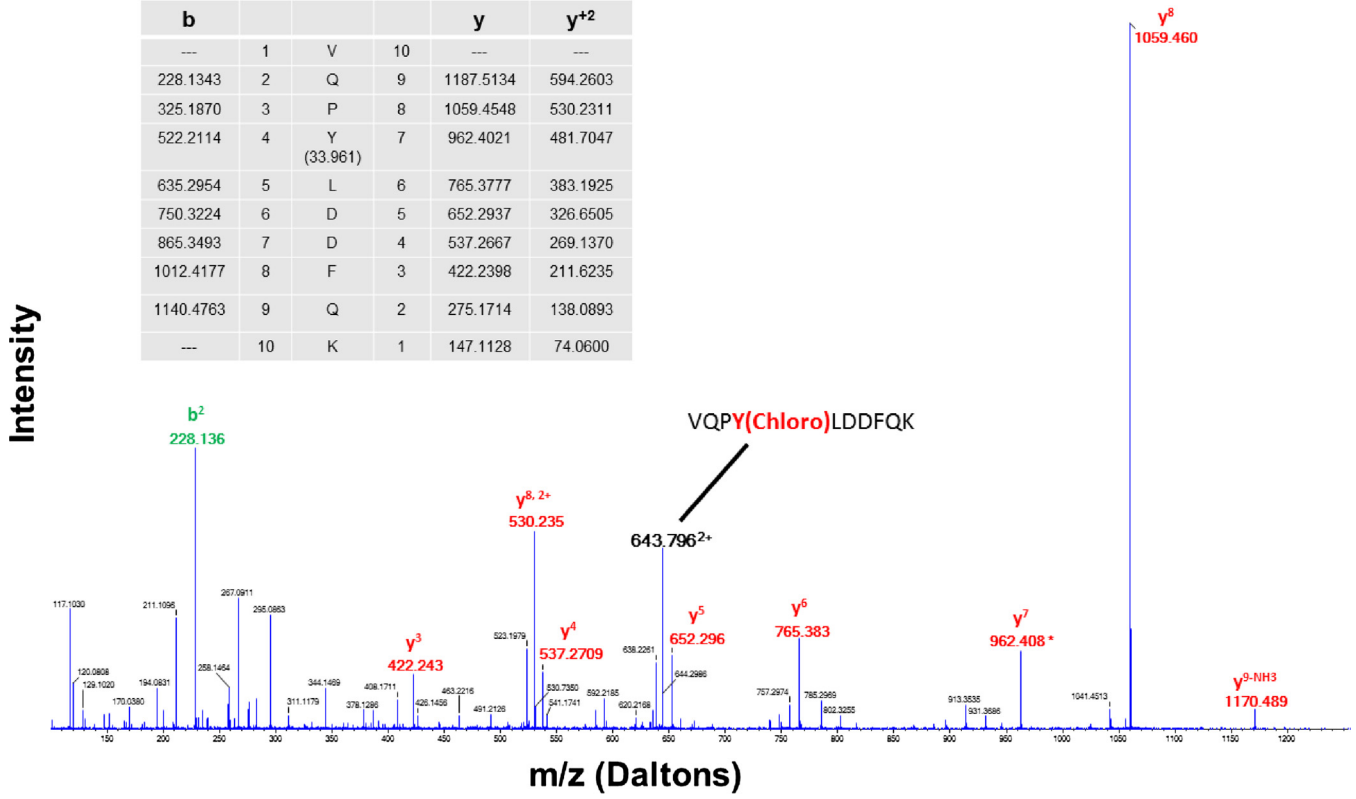

Fig. 4. MS/MS spectrum of hypochlorite-treated apoA-I. Analysis of the amino acid sequence of VQPYLDDFQK shows that addition of the tyrosine residue increases mass by 197 mass units. This is consistent with the addition of tyrosine (163 mass units) and a chlorine molecule (34 mass units).

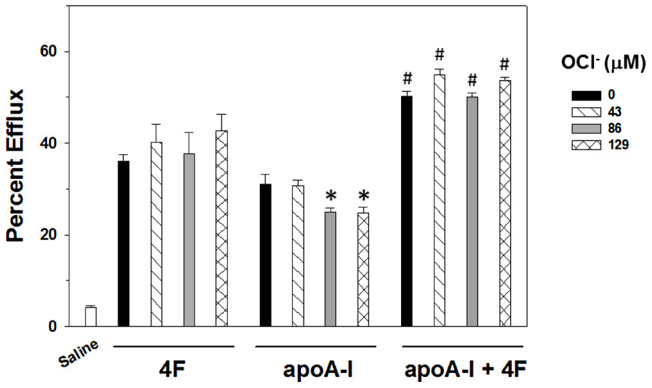

Fig. 5. Effects of hypochlorite on 4F and apoA-I mediated cholesterol efflux. ABCA1-dependent cholesterol efflux to 4F (100 μg/mL) or apoA-I (100 μg/mL) was measured in the presence of increasing concentrations of hypochlorite (OCl^-). Hypochlorite did not influence 4F-dependent efflux. In contrast, apoA-I mediated efflux was inhibited by 86 and 129μM hypochlorite. Mixing 4F and apoA-I resulted in a greater increase in cholesterol efflux than that seen with either treatment alone. Further, 4F abolished the inhibitory effect of hypochlorite on apoA-I -mediated cholesterol efflux. Data are the mean ± SEM (N = 6–12 per treatment group). * denotes a significant difference ($P < 0.05$) compared to apoA-I treatment with 0 or 43μM hypochlorite. # denotes a significant difference ($P < 0.05$) compared to the corresponding hypochlorite treatment of 4F or apoA-I alone.

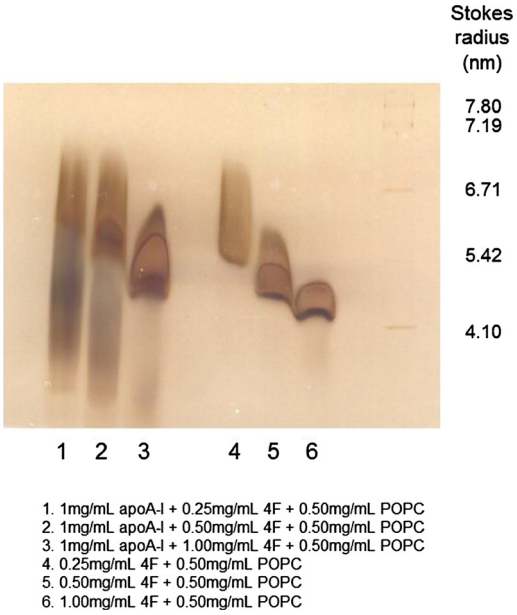

Fig. 6. 4F reacts with POPC to form particles of varying size. Addition of increasing concentrations of 4F (0.25–1.00 mg/mL) to a fixed amount of POPC (0.50 mg/ml) resulted in the formation of particles of smaller size. A similar response was observed when apoA-I was added to the reaction mixture. Under these conditions, particles of different size were formed.

hypochlorite was abolished in the presence of 4F. These data show that 4F prevents the hypochlorite-mediated inhibition of apoA-I function.

Results of non-denaturing gel electrophoresis studies (Fig. 6) showed that in the presence of a fixed amount of POPC, an increase in the concentration of 4F resulted in the formation of smaller particles. This trend was also present when 4F was incubated with POPC in the presence of apoA-I. Approximate stokes diameters of 4F:POPC particles are 6.1, 5.4 and 4.95 nm for 0.5:1, 1:1 and 2:1 ratios, respectively. Approximately two heterogeneous particles formed with apoA-I-4F-POPC at ratios 2:0.5:1, 2:1:1 and 2:2:1. All of these particles were different size than the particles formed by 4F:POPC. The larger particles were approximately 6.28, 6.1 and 5.4 nm, respectively, the smaller

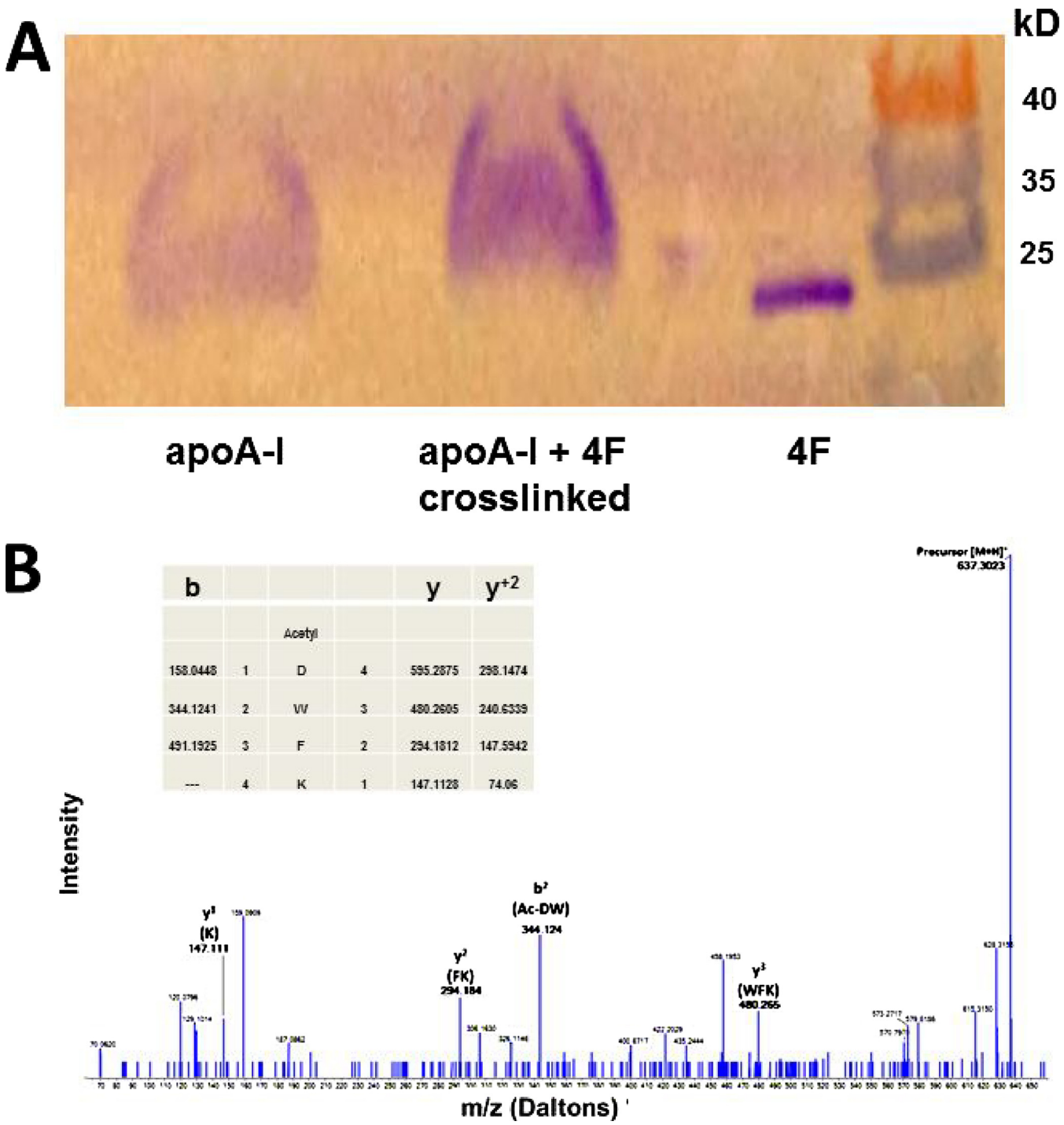

Fig. 7. Association of 4F and apoA-I. Crosslinking studies show that mixing 4F with apoA-I results in the formation of a larger particle (Panel A). MS/MS fragmentation spectrum of precursor ion 637.30 *m/z* representing a tryptic fragment of the acetylated 4F peptide. The collision-induced dissociation fragmentation clearly demonstrates the sequence of Ac-DWFK with b and y ion coverage. The b^2 ion of 344.124 *m/z* shows the addition of 42 Daltons of the acetyl group attached to the DW sequence at the N-terminus of the fragment (Panel B).

(diffused), heterogeneous particles are approximately 4.9, 4.58 and less than 4.58 nm.

Results of crosslinking studies (Fig. 7A) suggest that 4F and apoA-I are situated in close proximity in apoA-I -4F-POPC complexes. The crosslinked band formed by apoA-I and 4F is slightly higher in molecular weight, more intense than either 4F or apoA-I, suggesting apoA-I and 4F are both present in the different complexes. This was further confirmed by mass spectrometry studies. Crosslinked complexes of 4F and apoA-I (apoA-I:4F:POPC = 2:1:1 based on weight ratio) resolved on an SDS gel. The single band that ran slightly higher than either apoA-I of 4F was excised and subjected to tryptic digestion. Triple-TOF mass spectrometry revealed an association between 4F and apoA-I fragments (Fig. 7B).

Although apoA-I binds to POPC vesicles (Tricerri et al., 2002), it does not clarify POPC vesicles (Fig. 8). Addition of 1 mg of apoA-I to POPC MLVs (2.1 mg/3 ml PBS) for 30 min did not clarify POPC MLVs. However, addition of 4F to this complex at a ratio of 1:0.25 (apoA-I:4F w/w) initiated clarification, which increased with 4F concentration up

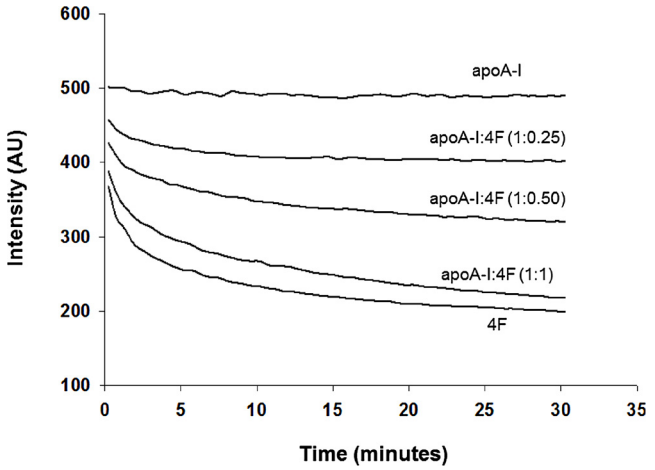

Fig. 8. Effect of 4F and apoA-I on the clarification of POPC MLVs. Addition of 1 mg of apoA-I to POPC MLVs (2.1 mg/3 ml) did not clarify the vesicles. In contrast, addition of 4F alone (1 mg) clarifies POPC vesicles. Addition of 4F at different concentrations (0.25 mg, 0.5 mg and 1 mg) caused a concentration-dependent increase in clarification.

to a 1:1 ratio (Fig. 8). We additionally observed that, at all ratios of apoA-I:4F, clarification of MLVs was complete after 24 h (not shown). As reported by us earlier, 4F (1 mg) alone causes clarification of POPC vesicles (Fig. 8) (Datta et al., 2001).

4. Discussion

Lipid free apoA-I associates with cell surface ABCA1 to form nascent nanoparticles, which act as carriers of cellular cholesterol. The property of apoA-I to associate with phospholipids in the presence of detergents has been utilized to form synthetic nanoparticles. Nanoparticles synthesized using apoA-I:POPC have been shown to protect against the development of atherosclerosis and diabetes in animal models. In addition, nanodisc systems have been used for both the discovery of new pharmacological agents as well as the therapeutic delivery of small molecule and protein based therapeutics (Shaw et al., 2008; Kenneth et al., 2011). ApoA-I can undergo oxidative modification in the presence of hypochlorite. This in turn reduces its biological properties, including ability to efflux cellular cholesterol. In addition, such particles may not be stable as carriers of pharmacological agents. 4F is an extensively studied apoA-I mimetic peptide and has shown to be highly effective in converting inflammatory HDL into an anti-inflammatory particle (Van Lenten et al., 2008; Navab et al., 2011b). 4F associates with oxidized lipids with high affinity compared to apoA-I (Van Lenten et al., 2008). Interestingly, hypochlorite oxidation of 4F did not alter its ability to efflux plasma cholesterol (White et al., 2012). Based on these observations, we hypothesized that presence of 4F would inhibit the hypochlorite-mediated oxidation of apoA-I. This may therefore stabilize and maintain the biological properties of apoA-I and nanoparticles containing apoA-I.

As shown in Figs. 1 and 2, hypochlorite-mediated oxidation of apoA-I was reduced in the presence of 4F. Proteins undergo dimerization upon tyrosine oxidation (Aeschbach et al., 1976). This indeed was the case, as seen in Fig. 1A, which shows an increase in the intensity of the band at 60 kD with 43 μM hypochlorite. This band and the apoA-I band densities disappeared with further increase of hypochlorite concentration. This process was prevented in the presence of 4F (Fig. 1B). Fig. 1C shows results of an average of seven experiments, clearly demonstrating that 4F significantly inhibits hypochlorite-mediated apoA-I oxidation. Mass spectrometry studies demonstrate that, in the presence of 4F, the hypochlorite-dependent modification of amino acid residues in apoA-I is reduced. 4F not only inhibited the hypochlorite-mediated oxidation of 4F, but also enhanced the ability of A-I to mediate ABCA1-dependent cholesterol efflux at all ratios of hypochlorite:apoA-I studied in this report compared to either apoA-I or 4F after hypochlorite-mediated oxidation. Since 4F by itself is quite effective in its ability to efflux cellular cholesterol *via* the ABCA1-mediated pathway, the observed results with apoA-I in the presence of 4F could be the additive property of apoA-I and 4F. In any case, the presence of 4F exerted a beneficial effect on cholesterol effluxing properties of apoA-I.

Since apoA-I does not associate with POPC in the absence of detergents, we added increasing amounts of 4F to the apoA-I:POPC mixture. Fig. 8 shows the effect of 4F on the ability of apoA-I to solubilize POPC. The complexes formed by 4F-apoA-I -POPC are heterogeneous as shown in Fig. 6. To establish that both 4F and apoA-I are present in all of the complexes shown in Fig. 6, we cross-linked the complexes formed by apoA-I -4F-POPC at 1:0.5:0.5 (weight) ratio, ran on an SDS gel, excised the single band that in size is different from either 4F and apoA-I. The band was subjected to MS/MS analysis. Results (Fig. 7) showed the presence of 4F. We also did not see any bands due to either 4F or apoA-I. These results suggest that all of the particles possessed both apoA-I and 4F. Detailed studies are underway to establish the ratio of apoA-I and 4F in different bands. Additional studies are also required to determine the nature and biological properties of different complexes shown in Fig. 6. 4F:POPC complexes have been shown to interact with and solubilize membrane proteins (Barnaba et al., 2018a; Prade et al., 2018; Barnaba et al., 2018b). In this context, we reported that 4F or 4F:lipid complexes inhibit Alzheimer's disease and amyloid beta fibril formation (Sahoo et al., 2018; Handattu et al., 2009).

ApoA-I-containing nanoparticles have been used in preclinical studies as vehicles to deliver molecules directly to the cytoplasm of certain cancer cells (*Nissen et al., 2003;Kenneth et al., 2011*). To form these nanoparticles, one has to use a detergent such as cholate, which eventually has to be dialyzed (Bayburt et al., 2002; Denisov et al., 2004). As shown in Fig. 6, apoA-I:lipid complexes can be formed by adding a small amount of 4F. Considering both apoA-I:lipid complexes and 4F have been shown to possess remarkable protective properties and act as carriers of small molecules and drugs, we propose that nanoparticles containing both 4F and apoA-I can be formed even in the absence of detergents. These complexes would be most beneficial either as agents to ameliorate lipid-mediated disorders or as nanoparticles to carry hydrophobic therapeutic agents to the site of disease in a soluble form.

Conflict of interest

None.

Acknowledgement

This work was supported by grants from the National Institutes of Health (GM115367 and DK108836).

References

Aeschbach, R., Amado, R., Neukon, H., 1976. Formation of dityrosine cross-links in proteins by oxidation of tyrosine residues. Biochim. Biophys. Acta 439, 292–301.
Anantharamaiah, G.M., Garber, D.W., 1996. Chromatographic methods for quantitation of apolipoprotein A-I. Methods Enzymol. 263, 267–282.
Anantharamaiah, G.M., Hughes, T.A., Iqbal, M., Gawish, A., Neame, P.J., Medley, M.F., Segrest, J.P., 1988. Effect of oxidation on the properties of apolipoproteins A-I and A-II. J. Lipid Res. 29, 309–318.
Barnaba, C., Ravula, T., Medina-Meza, I.G., Im, S.C., Anantharamaiah, G.M., Waskell, L., Ramamoorthy, A., 2018a. Lipid-exchange in nanodiscs discloses membrane boundaries of cytochrome-P450 reductase. Chem. Commun. (Camb.) 14 (54), 6336–6339.
Barnaba, C., Sahoo, B.R., Ravula, T., Medina-Meza, I.G., Im, S.C., Anantharamaiah, G.M., Waskell, L., Ramamoorthy, A., 2018b. Cytochrome-P450-induced ordering of microsomal membranes modulates affinity for drugs. Angew. Chem. Int. Ed. Engl. 57, 3391–3395.
Bayburt, T.H., Grinkova, Y.V., Sligar, S.G., 2002. Self-assembly of discoidal phospholipid bilayer nanoparticles with membrane scaffold proteins. Nanoletters 2, 853–856.
Chung, B.H., Segrest, J.P., Ray, M.J., Brunzell, J.D., Hokanson, J.E., Krauss, R.M., Beaudrie, K., Cone, J.T., 1996. Single vertical spin density gradient

ultracentrifugation. Methods Enzymol. 128, 181–263.
D'Silva, R.A.G., Hilliard, G.M., Ling, Li, Segrest, J.P., Davidson, W.S., 2005. Mass spectrometric determination of the conformation of dimeric apolipoprotein A-I in discoidal high density lipoproteins. Biochemistry 44, 8600–8607.
Datta, G., Chaddha, M., Hama, S., Navab, M., Fogelman, A.M., Garber, D.W., Mishra, V.K., Epand, R.M., Epand, R.F., Lund-Katz, S., Phillips, M.C., Segrest, J.P., Anantharamaiah, G.M., 2001. Effects of increasing hydrophobicity on the physical-chemical and biological properties of a class A amphipathic helical peptide. J. Lipid Res. 42, 1096–1104.
Datta, G., Epand, R.F., Epand, R.M., Chaddha, M., Kirksey, M.A., Garber, D.W., Lund-Katz, S., Phillips, M.C., Hama, S., Navab, M., Fogelman, A.M., Palgunachari, M.N., Segrest, J.P., Anantharamaiah, G.M., 2004. Aromatic residue position on the non-polar face of Class A amphipathic helical peptides determines biological activity. J. Biol. Chem. 279, 26509–26517.
Denisov, I.G., Grinkova, Y.V., Lazarides, A.A., Sligar, S.G., 2004. Directed self-assembly of monodisperse phospholipid bilayer nanodiscs with controlled size. J. Am. Chem. Soc. 126, 3477–3487.
Gorden, T., Castelli, W.P., Hjortland, Kannell, W.B., Dawber, T.R., 1977. High density lipoprotein as a protective factor against coronary heart disease. The Framingham Study. Am. J. Med. 62, 707–714.
Handattu, S.P., Garber, D.W., Monroe, C.E., van Groen, T., Kadish, I., Nayyar, G., Cao, D., Palgunachari, M.N., Li, L., Anantharamaiah, G.M., 2009. Oral apolipoprotein A-I mimetic peptide improves cognitive function and reduces amyloid burden in a mouse model of Alzheimer's disease. Neurobiol. Dis. 34, 525–534.
Ibanez, B., Giannarelli, C., Cimmino, G., Santos-Gallego, C.G., Alique, M., Pinero, A., Vilahur, G., Fuster, V., Badimon, L., Badimon, J.J., 2012. Recombinant HDL(Milano) exerts greater anti-inflammatory and plaque stabilizing properties than HDL(wild-type). Atherosclerosis 220, 72–77.
Jin, H., Lovell, J., Chen, J., Ng, K., Cao, W., Ding, L., Zhang, Z., Zheng, G., 2010. Investigating the specific uptake of EGF-conjugated nanoparticles in lung cancer cells using fluorescence imaging. Cancer Nanotechnol. 1, 71–78.
Kenneth, K., Jonathan, N.G., Lovell, F., 2011. Lipoprotein-inspired nanoparticles for cancer theranostics. Acc. Chem. Res. 44, 1105–1113.
Kingwell, B.A., Chapman, M.J., Kontush, A., Miller, N.E., 2014. HDL-targeted therapies: progress, failures and future. Nat. Rev. Drug Discov. 13, 445–464.
Kritharides, L., Christian, A., Stoudt, G., Morel, D., Rothblat, G.H., 1998. Cholesterol metabolism and efflux in human THP-1 macrophages. Arterioscler. Thromb. Vasc. Biol. 18, 1589–1599.
Navab, M., Anantharamaiah, G.M., Fogelman, A.M., 2008. The effect of apolipoprotein mimetic peptides in inflammatory disorders other than atherosclerosis. Trends Cardiovasc. Med. 18, 61–66.
Navab, M., Shechter, I., Anantharamaiah, G.M., Reddy, S.T., Van Lenten, B.J., Fogelman, A.M., 2010. Structure and function of HDL mimetics. Arterioscler. Thromb. Vasc. Biol. 30, 164–168.
Navab, M., Reddy, S.T., van Lenten, B.J., Fogelman, A.M., 2011a. HDL and cardiovascular disease: atherogenic and atheroprotective mechanisms. Nat. Rev. Cardiol. 8, 222–232.
Navab, M., Reddy, S.T., Anantharamaiah, G.M., Imzmi, S.S., Fogelman, A.M., 2011b. Intestine may be a major site of action for the apoA-I mimetic peptide 4F whether administered subcutaneously or orally. J. Lipid Res. 52, 1200–1210.
Nissen, S.E., Tsunoda, T., Tuzcu, E.M., Schoenhagen, P., Cooper, C.J., Yasin, M., Eaton, G.M., Lauer, M.A., Sheldon, W.S., Grines, C.L., Halpern, S., Crowe, T., Blankenship, J.C., Kerensky, R., 2003. Effect of recombinant apoA-I milano on coronary atherosclerosis in patients with acute coronary syndromes: a randomized controlled trial. JAMA 290, 2292–2300.
Prade, E., Mahajan, M., Im, S.C., Zhang, M., Gentry, K.A., Anantharamaiah, G.M., Waskell, L., Ramamoorthy, A., 2018. A minimal functional complex of cytochrome P450 and FBD of cytochrome P450 reductase in nanodiscs. Angew. Chem. Int. Ed. Engl. 57, 8458–8462.
Reddy, S.T., Navab, M., Anantharamaiah, G.M., Fogelman, A.M., 2013. Searching for a successful HDL-based treatment strategy. Biochim. Biophys. Acta 1841 (1), 162–167.
Rye, K.-A., Bursill, C.A., Lambert, G., Tabet, F., Barter, P.J., 2009. The metabolism and anti-atherogenic properties of HDL. J. Lipid Res. 50, S195–S200.
Sahoo, B.R., Genjo, T., Cox, S.J., Stoddard, A.K., Anantharamaiah, G.M., Fierke, C., Ramamoorthy, A., 2018. Nanodisc-forming scaffold protein promoted retardation of amyloid-beta aggregation. J. Mol. Biol. 430, 4230–4244.
Shah, P.K., Yano, J., Reyes, O., Chyu, K.Y., Kaul, S., Bisgaier, C.L., Drake, S., Cercek, B., 2001. High-dose recombinant apolipoprotein A-I(milano) mobilizes tissue cholesterol and rapidly reduces plaque lipid and macrophage content in apolipoprotein E-deficient mice. Potential implications for acute plaque stabilization. Circulation 103, 3047–3050.
Shaw, J.A., Bobik, A., Murphy, A., Kanellakis, P., Blombery, P., Mukhamedova, N., Woollard, K., Lyon, S., Sviridov, D., Dart, A.M., 2008. Infusion of reconstituted high-density lipoprotein leads to acute changes in human atherosclerotic plaque. Circ. Res. 103, 1084–1091.
Skajaa, T., Zhao, Y., van den Heuvel, D.J., Gerritsen, H.C., Cormode, D.P., Koole, R., van Schooneveld, M.M., Post, J.A., Fisher, E.A., Fayad, Z.A., de Mello Donega, C., Meijerink, A., Mulder, W.J.M., 2010. Quantum dot and Cy5.5 labeled nanoparticles to investigate lipoprotein biointeractions via F€orster resonance energy transfer. ACS Nano 10, 5131–5138.
Sorci-Thomas, M.G., Curtiss, L., Parks, J.S., Thomas, M.J., Kearns, M.W., 1997. Alteration in Apolipoprotein A-I 22-mer repeat order results in a decrease in lecithin:cholesterol acyltransferase reactivity. J. Biol. Chem. 272, 7278–7284.
Tardif, J.C., Gregoire, J., L'Allier, P.L., Ibrahim, R., Lesperance, J., Heinonen, T.M., Kouz, S., Berry, C., Basser, R., Lavoie, M.A., Guertin, M.C., Rodes-Cabau, J., 2007. Effects of reconstituted high-density lipoprotein infusions on coronary atherosclerosis: a randomized controlled trial. JAMA 297, 1675–1682.
Tricerri, M.A., Sanchez, S.A., Arnulphi, C., Durbin, D.M., Gratton, E., Jonas, A., 2002. Interaction of apolipoprotein A-I in three different conformations with palmitoyl oleoyl phophatidylcholine vesicles. J. Lipid Res. 43, 187–197.
Van Lenten, B.J., Hama, S.Y., de Beer, F.C., Stafforini, D.M., McIntyre, T.I., Prescott, S.M., La Du, B.N., Fogelman, A.M., Navab, M., 1995. Anti-inflammatory HDL becomes pro-inflammatory during the acute phase response. Clin. Invest. 96, 2758–2767.
Van Lenten, B.J., Wagner, A.C., Jung, C.-L., Ruchala, P., Waring, A.J., Lehrer, R.I., Watson, A.D., Hama, S., Navab, M., Anantharamaiah, G.M., Fogelman, A.M., 2008. Anti-inflammatory apoA-I-mimetic peptides bind oxidized lipids with much higher affinity than human apoA-I. J. Lipid Res. 49, 2302–2311.
White, C.R., Datta, G., Buck, A.K., Chaddha, M., Reddy, G., Wilson, L.M., Palgunachari, M.N., Abbasi, M., Anantharamaiah, G.M., 2012. Preservation of biological function despite oxidative modification of the apolipoprotein A-I mimetic peptide 4F. J. Lipid Res. 53, 1576–1587.
White, C.R., Garber, D.W., Anantharamaiah, G.M., 2014. Anti-inflammatory and cholesterol-reducing properties of apolipoprotein mimetics. J. Lipid Res. 55, 2007–2021.
Zhang, Z., Cao, W., Jin, H., Lovell, J.F., Yang, M., Ding, L., Chen, J., Corbin, I., Luo, Q., Zheng, G., 2009. Biomimetic nanocarrier for direct cytosolic drug delivery. Angew. Chem. Int. Ed. 48, 9171–9175.